

# Reactions in lipid vesicles. Pyrene excimer formation in restricted geometries. Effect of temperature and concentration

P. Lianos<sup>1</sup> and G. Duportail<sup>2</sup>

<sup>1</sup> School of Engineering, University of Patras, 2600 Patras, Greece

<sup>2</sup> Centre de Recherches Pharmaceutiques, Laboratoire de Physique, U.A. CNRS 491, Université Louis Pasteur, P.O. Box 24, F-67401 Illkirch Cedex, France

Received March 22, 1991/Accepted November 28, 1991

**Abstract.** The decay of pyrene in the presence of excimers in small unilamellar vesicles of 3-sn-phosphatidyl glycerol, dipalmitoyl and 3-sn-phosphatidylglycerol from egg yolk has been analyzed with the use of models appropriate for reactions in restricted geometries. Results are presented with emphasis on probe concentration and temperature. The reaction rate in an organized lipid phase is redefined in a simple manner which allows for a simple treatment of any reaction in such environments. The analysis allows detection of pyrene aggregation in the vesicle lipidic core.

**Key words:** Phospholipid vesicles – Restricted geometries – Pyrene excimer

## Introduction

The study of reactions in lipid vesicles is of great importance both from the fundamental and the biophysical point of view. Lipid vesicles provide a particular environment with low-dimensional geometry. The effects of dimensionality on chemical reactions are currently treated with kinetic models obtained from the theory of random walks in fractal domains (Takami and Mataga 1987; Yamazaki et al. 1990; Kopelman 1986; Meakin and Stanley 1984; Argyrakis and Kopelman 1987; Lopez-Quintela et al. 1987, 1989; Lianos 1988; Duportail and Lianos 1988, 1990). In the present work we employ fluorescence probing, by using the extensively studied fluorophore pyrene, to model the reaction  $A + B \rightarrow \text{products}$  ( $[A] \ll [B]$ ) in lipid vesicles. In fact, A corresponds to excited and B to unexcited pyrene molecules in a usual excimer-forming reaction. The concentration of excited pyrene is monitored by time-resolved fluorescence and the models used for analysis are written for such processes.

The excimer forming reaction in the lipid bilayer may or may not be a diffusion-controlled process. In any case, the reaction rates are expected to depend explicitly on the

distance  $r_i$  between the excited fluorophore and the  $i$ th quencher (here the unexcited pyrene molecule). We have previously shown (Lianos 1988; Duportail and Lianos 1988) by an analysis based on the work of Allinger and Blumen (1980), that these distance (and time)-dependent rates yield a fluorescence decay profile described by an infinite product of stretched exponentials. However, in a practical analysis the infinite number of factors is well approximated by only two, as shown in the following equation:

$$I(t) = I_0 \exp(-k_0 t) \exp(-C_1 t^f + C_2 t^{2f}) \quad (1)$$

where  $k_0$  is the decay rate constant in the absence of quenching,  $C_1$  and  $C_2$  are constants and  $f$  is a non-integer, positive exponent, smaller than unity, proportional to the dimensionality of the reaction domain.

If the reaction between the excited fluorophore and the quencher is modelled as a random walk then  $f$  has an additional interesting feature. In random-walk terms, the reaction rate depends on the number of distinct sites  $S(n)$  visited by the random walker performing  $n$  steps, which is given by  $S(n) \sim n^f$ , where  $f = d_s/2 = d_f/d_w$ .  $d_s$  is then the spectral dimension,  $d_f$  the fractal dimension and  $d_w$  the fractal dimension of the random walk (Rammal and Toulouse 1983; Havlin and Ben-Avraham 1987; Kopelman 1986; Klafter and Blumen 1984). In this case, the term  $C_1 t^f$  is proportional to the average  $S(t)$  while  $C_2 t^{2f}$  is proportional to its variance (Klafter and Blumen 1984).

The equivalent first-order reaction rate “constant”  $K(t)$  is not constant but is obtained through the following equation:

$$K(t) = \frac{f C_1}{t^{1-f}} - \frac{2 f C_2}{t^{1-2f}} \quad (2)$$

The equivalent second-order rate “constant” can be obtained by the simple relation

$$k(t) = \frac{K(t)}{[P]} \quad (3)$$

where  $[P]$  is the total pyrene concentration.

Equation (1) successfully describes the decay of monomer pyrene in the presence of excimers in the lipid bilayer (Duportail and Lianos 1988 and 1990). The analysis of the monomer decay profiles allows the calculation of the parameters  $C_1$ ,  $C_2$  and  $f$  and through (2) the reaction rate  $K(t)$ . In the present work we systematically apply the above theory to study pyrene excimer formation by controlling various factors which allow correct application of (1) through (3) and allow extraction of important information on the vesicle-probe system. In particular, two types of vesicles composed of single phospholipid species were studied, i.e. 3-sn-phosphatidylglycerol, dipalmitoyl (DPPG) and 3-sn-phosphatidylglycerol prepared from egg yolk (EPG). The fluorescence decays were measured in the temperature range  $10^\circ$ – $30^\circ\text{C}$ , ensuring that DPPG vesicles are always in the gel phase and EPG vesicles in the liquid crystalline phase. The temperature was varied between these limits in order to detect a possible temperature effect in a monophasic system, whereas the probe-concentration dependence was studied by varying it from  $10^{-6}$  to  $3 \times 10^{-5}$  M. Small unilamellar vesicles were used in order to reduce the scattered light due to the vesicles, though it cannot be completely eliminated.

Pyrene has been previously used to probe the structure and dynamics of phospholipid vesicles (see Daems et al. 1985; L'Heureux and Fragata 1989). The analysis of the fluorescence decay profiles of pyrene, which is also the main topic of the present work, has been done either by fitting a sum of exponentials (Liu et al. 1980) or by utilizing a time-dependent diffusion coefficient based on the Einstein-Smoluchowski diffusion theory (Vanderkooi and Callis 1974). A controversy has arisen as to which of the two models might be appropriate, since diffusion-controlled excimer formation of pyrene in phospholipid vesicles is in some cases questioned (Blackwell et al. 1986; L'Heureux and Fragata 1989). The present work sheds some light on this question while it introduces the concept of dimensionality into the employed mathematical models.

## Materials and methods

3-sn-phosphatidylglycerol, dipalmitoyl (DPPG) and 3-sn-phosphatidylglycerol (EPG) prepared from egg yolk were obtained from Sigma (ref. P 2892 and P 0514, respectively) and used without further purification. These anionic phospholipids were used because the resulting vesicles were much less turbid than vesicles obtained from phosphatidylcholine. Small unilamellar vesicles were prepared as previously described (Duportail and Lianos, 1990) in a phosphate buffer (100 mM) at pH 7. The average diameter of these vesicles, measured by photon-correlation spectroscopy, was 70 nm. Each sample was characterized by phospholipid and pyrene concentrations. The phospholipid concentration was inferred from the concentration of its stock solution in chloroform, according to Bartlett (1959). Concentrations of pyrene embedded into the vesicles were checked both by absorption and fluorescence spectrophotometry, and were expressed as

the total macroscopic concentration. We have actually used two phospholipid concentrations, i.e.  $3.5 \times 10^{-4}$  and  $10^{-4}$  M, while the pyrene concentration varied from  $<10^{-6}$  M to  $3 \times 10^{-5}$  M in the first case and from  $<10^{-6}$  M to  $2 \times 10^{-5}$  M in the second case.

The fluorescence decay curves were recorded with a time-correlated photon-counting apparatus equipped with a high-pressure hydrogen flash (8 bars). The excitation wavelength (321 nm) was selected by a Bausch-Lomb monochromator. The monomer pyrene fluorescence emission was selected by a 385 nm Schott interference filter. To avoid quenching by oxygen, all samples were deoxygenated by bubbling nitrogen for 30 min, before measurements. The decay time of pyrene monomer (without excimer) was measured on samples having a pyrene concentration low enough ( $<10^{-6}$  M) to preclude excimer formation. The fluorescence decay profiles were analyzed with least-square fits using the distribution of the residuals and the autocorrelation function of the residuals as fitting criterion. Chi-square values have also been calculated and they are tabulated with the other data. The number of peak counts was around 30,000. The time-profile of the excitation pulse (see Fig. 1) was judged to be wide enough to necessitate convolution of the applied model. In fact, (1) was used in the following form

$$F_i = A \left[ \sum_{j=1}^i G_j \exp \{ -k_0 w(i-j) \} \cdot \exp \{ -C_1 [w(i-j)]^f + C_2 [w(i-j)]^{2f} \} \right] \quad (4)$$

where  $F_i$  corresponds to the experimental value of the fluorescence intensity at channel  $i$ ,  $A$  is a fitted parameter,  $G_j$  is the value of the intensity of the exciting pulse at channel  $j$  and  $w$  is the time-interval between two channels (presently 1.87 ns). The fitting started 38 channels after the point where the exciting pulse starts rising, in order to

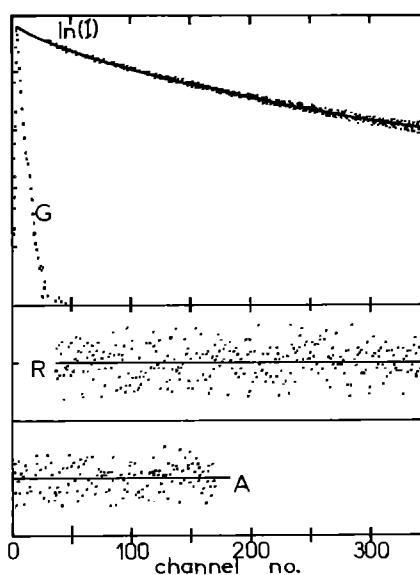


Fig. 1. Monomer fluorescence decay profile of  $2 \times 10^{-5}$  M pyrene solubilized in  $3.5 \times 10^{-4}$  M DPPG at  $20^\circ\text{C}$ , together with fitted curve, exciting pulse (G), residuals (R) and autocorrelation function of the residuals (A). The fitted model was in the form of (4)

avoid interference from scattered light. Of course, this choice is made at some expense of the information which is contained in these first 38 channels. However, we believe that it does not dramatically affect our results. At any rate, the scattered light interference would have produced much greater error. The analysis was done individually for each decay curve (no global analysis).

Diphenylhexatriene (DPH, from Koch-Light, scintillation grade) was used as a viscosity fluorescent probe and was incorporated in the vesicles in the same way as pyrene (Duportail and Lianos 1990). The fluorescence anisotropy of the DPH-labelled vesicles was measured with a SLM-8000 spectrofluorometer in the T-format ( $\lambda_{\text{exc}} = 360$  nm,  $\lambda_{\text{em}} = 435$  nm).

## Results and discussion

Pyrene was first solubilized in small unilamellar vesicles of DPPG. The steady-state fluorescence spectra are shown in Fig. 2 for two extreme concentrations of the fluorophore. With a small pyrene concentration, the monomer lifetime  $\tau_0$  ( $=1/k_0$ ) in the absence of excimer was shown to vary between 345 and 277 ns when the temperature varied between 10 and 30°C (see Table 1, cf. Daems et al. 1985). When the pyrene concentration was above  $10^{-6}$  M, excimer was formed in the vesicle bilayer while the fluorescence decay profile could be fitted with the exclusive use of (4). The results obtained for some pyrene concentrations are shown in Table 1 vs.  $T$ . The temperature range of 10–30°C was chosen in order to obtain single-phase vesicles. In fact the fluorescence anisotropy  $r$  of diphenylhexatriene solubilized in small unilamellar vesicles of DPPG changes very little in the above temperature range (Table 1).  $r$  would have decreased abruptly if a gel to liquid crystalline phase transition had occurred. In the case of DPPG, this phase transition appears only at 41°C.

$\tau_0$  decreases with increasing temperature. This is expected, since non-radiative decay processes are enhanced at higher temperatures. The non-integer exponent  $f$  increased with temperature while the values of the constants  $C_1$  and  $C_2$  decreased with temperature (Table 1).  $C_1$ ,  $C_2$  and  $f$  were used to monitor the form of the time-dependent reaction rate according to (2) and (3). Figure 3 shows some examples of the way  $k(t)$  evolves with time.  $k(t)$  decreases fast at short times to reach an almost constant value at later times. The value of  $k(t)$  at the 400th channel (last channel of observation, 1.87 ns/channel) was always found to be zero within experimental error. Because of the variation of  $k(t)$  with time we have chosen to tabulate two of its representative values for each set  $C_1$ ,  $C_2$  and  $f$ , i.e. its value  $k_1$  (channel no. 1) and its average  $k_{av}$  over a period of 400 channels.  $k(t)$  shows a different variation pattern vs.  $T$  at different times. Thus at the end of the observation period it is practically zero, which suggests that in DPPG vesicles the excimer reaction is completed within a relatively short time, compared with the total time-range of observation. In other words, quenchers lying at relatively long distances have no chance to reach the excited pyrene within its excited-state lifetime.

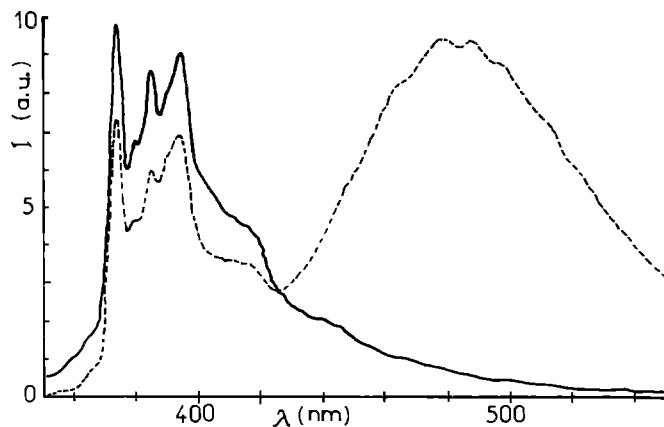


Fig. 2. Fluorescence spectra of pyrene in  $10^{-4}$  M DPPG at 20°C: —  $10^{-6}$  M; - - -  $2 \times 10^{-5}$  M.  $\lambda_{\text{exc}} = 321$  nm

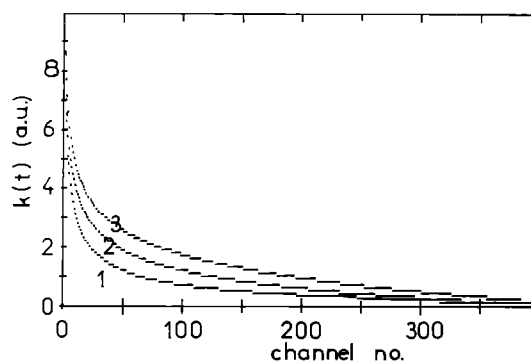


Fig. 3. Variation of  $k(t)$  with time at three different values of  $f$ . All data correspond to  $2 \times 10^{-5}$  of pyrene solubilized in  $3.5 \times 10^{-4}$  M DPPG: (1)  $T = 10^\circ\text{C}$ ,  $f = 0.54$ ; (2)  $T = 20^\circ\text{C}$ ,  $f = 0.65$ ; and (3)  $T = 30^\circ\text{C}$ ,  $f = 0.71$

Table 1. Values of  $r$ ,  $\tau_0$ ,  $C_1$ ,  $C_2$ ,  $f$ ,  $\chi^2$ ,  $k^1$  and  $k_{av}$  vs  $T$  for three pyrene concentrations and  $3.5 \times 10^{-4}$  M DPPG

$T$ (°C)	$r$	$\tau_0$ (ns)	$10^3 C_1^a$	$10^5 C_2^a$	$f$	$\chi^2$	$K_1$ ( $10^{11} \text{ M}^{-1} \text{ s}^{-1}$ )	$k_{av}^b$
[P] = $5 \times 10^{-6}$ M								
10	0.34	345	17	22	0.59	1.00	15	0.8
20	0.33	304	13	13	0.65	1.04	13	0.7
30	0.31	277	14	43	0.68	1.45	15	2.3
[P] = $10^{-5}$ M								
10	0.34	345	85	138	0.49	1.09	29	1.6
15	0.34	320	65	85	0.53	1.00	25	1.6
20	0.33	304	47	43	0.60	1.00	21	1.7
25	0.33	290	38	28	0.63	1.18	19	1.7
30	0.31	277	21	9	0.73	1.12	13	1.6
[P] = $2 \times 10^{-5}$ M								
10	0.34	345	63	74	0.54	1.01	12	0.8
15	0.34	320	36	26	0.63	1.00	9	0.8
20	0.33	304	38	25	0.65	1.03	10	1.0
25	0.33	290	29	14	0.70	1.03	8	1.0
30	0.31	277	30	12	0.71	1.13	9	1.2

<sup>a</sup> No units can be ascribed to  $C_1$  and  $C_2$  because of time being raised to a non-integer, variable value

<sup>b</sup> The average rate was calculated over 400 channels (1.87 ns/channel)

This situation is not affected by varying temperature in the above specified range. The rate constant  $k_1$  decreases while the average values  $k_{av}$  tends to increase with increasing temperature.

The variation trends for  $f$ ,  $k_1$  and  $k_{av}$  can be explained as follows. The average reaction rate tends to increase with temperature as usually happens with any diffusion-controlled reaction. Since  $f$  is an exponent proportional to the dimensionality of the reaction domain, it measures the extent of geometrical restrictions imposed on the reaction, therefore its increase with temperature marks a relaxation of the imposed restrictions. It is worth noting at this point a work by Blumen et al. (1988) where a theoretical basis of the increase of the exponent  $f$  with temperature is given. The variation of  $f$  affects the time-evolution of the rate  $k(t)$ . The decrease of  $k(t)$  with temperature at short times is related to the effect of temperature on probe distribution. For a given pyrene concentration in a given vesicle solution, the probability of an immediate encounter between reactants right-after excitation, decreases with increasing temperature. In other words, the reactants are expected to be more dispersed at higher temperatures. However, higher temperatures facilitate diffusion allowing for higher rates in the largest part of the time domain, as seen by the values of  $k_{av}$ . The second-order rates  $k_1$  and  $k_{av}$  have relatively high values (of the order of  $\geq 10^{11} \text{ M}^{-1} \text{ s}^{-1}$ ) much higher than the corresponding values in other organized assemblies (such as micelles). This is due to the high efficiency of the reaction owing to high local concentrations (only  $2 \times 10^{-5} \text{ M}$  pyrene in vesicles already gives a lot of excimer, cf. Fig. 2).

Table 2 shows similar data obtained at a given temperature ( $20^\circ\text{C}$ ) for pyrene concentration varying between  $5 \times 10^{-6}$  and  $3 \times 10^{-5} \text{ M}$  and for two different DPPG concentrations ( $10^{-4} \text{ M}$  and  $3.5 \times 10^{-4} \text{ M}$ ). Table 2 gives the values of the  $k$ 's but also the values of the products  $k[P]$  which correspond to an equivalent first-order rate

**Table 2.** Values of  $C_1$ ,  $C_2$ ,  $f$ ,  $\chi^2$ ,  $K_1$ ,  $K_{av}$ ,  $k_1$ ,  $k_{av}$  vs pyrene concentration for two DPPG concentrations:  $10^{-4}$  and  $3.5 \times 10^{-4} \text{ M}$  at  $20^\circ\text{C}$  ( $\tau_0 = 304 \text{ ns}$  in all cases)

Pyrene concentration ( $10^{-6} \text{ M}$ )	$10^3 C_1^a$	$10^5 C_2^a$	$f$	$\chi^2$	$K_1$ ( $10^6 \text{ s}^{-1}$ )	$K_{av}^b$ ( $10^6 \text{ s}^{-1}$ )	$k_1$ ( $10^{11} \text{ M}^{-1} \text{ s}^{-1}$ )	$k_{av}^b$ ( $10^{11} \text{ M}^{-1} \text{ s}^{-1}$ )
<b><math>10^{-4} \text{ M DPPG}</math></b>								
5	42	46	0.56	1.32	17	1.3	34	2.5
10	148	250	0.45	1.02	46	2.5	46	2.5
20	537	2,600	0.35	1.19	112	3.2	56	1.6
<b><math>3.5 \times 10^{-4} \text{ M DPPG}</math></b>								
5	13	13	0.65	1.04	7	0.4	13	0.7
10	47	43	0.60	1.00	21	1.7	21	1.7
15	35	31	0.61	1.00	16	1.3	11	0.8
20	38	25	0.65	1.03	20	2.0	10	1.0
30	53	39	0.62	1.05	26	2.4	10	0.8

<sup>a</sup> No units can be ascribed to  $C_1$  and  $C_2$  because of time being raised to a non integer, variable value

<sup>b</sup> The average rate was calculated over 400 channels (1.87 ns/channel)

“constant”  $K(t)$ . Both  $k(t)$  and  $K(t)$  were practically zero at the 400th channel in accordance with the findings in Table 1. Then in small unilamellar vesicles of DPPG there is no interaction at relatively long times. Both  $K_1$  and  $K_{av}$  increased with pyrene concentration in all cases examined. The formation then of pyrene excimers is facilitated at higher probe concentration. The variation trends of  $k_1$  and  $k_{av}$  with pyrene concentration can be explained in conjunction with the behavior of the values of the non-integer exponent  $f$ . The latter decreases with increasing pyrene concentration in the case of low lipid concentration ( $10^{-4} \text{ M}$ ) but stays practically invariant in the case of high lipid concentration ( $3.5 \times 10^{-4} \text{ M}$ ). It is, in the first place, a little surprising that for one pyrene molecule per five phospholipid molecules (i.e.  $2 \times 10^{-5}/10^{-4} \text{ M}$ , first case) we get a vast decrease of  $f$ , while for one pyrene molecule per about twelve phospholipids (i.e.  $3 \times 10^{-5} \text{ M}/3.5 \times 10^{-4} \text{ M}$ , second case) there is practically no change of  $f$ . This important finding may suggest the existence of lipid concentration effects on the structure of the small unilamellar vesicles obtained and the behavior of pyrene solubilized there. At any rate, the pyrene to lipid ratios used here are high. Therefore the vesicles must be highly perturbed by the presence of pyrene so that unusual effects can be observed. The invariance of  $f$  with pyrene concentration in  $3.5 \times 10^{-4} \text{ M DPPG}$  is considered here a normal case of pyrene excimer formation in the hydrophobic environment provided by the lipid vesicles. Such invariance is justified by model systems studied by computer simulations (Argyris et al. 1991). When, however, the lipid concentration decreases substantially, the variation of  $f$  values revealed an increasing compactness of the reaction (of the random walk) with increasing concentration. At small lipid (and vesicle) concentration, the number of pyrene molecules solubilized in the same vesicles is relatively high. Then it is possible to obtain an excited pyrene molecule in the close vicinity of an unexcited one and the excimer formation to be facilitated so to appear as static. The “dynamic” aspect of such a quasi-static interaction is a fast decrease of fluorescence intensity leading to a steeper descent of the decay profile. In such cases  $f$ -values appear smaller. Of course, this phenomenon is favored at higher pyrene concentrations. We believe that small  $f$ -values appearing at higher reactant concentrations do not reflect the geometry of the reaction domain but rather the geometry of the solubilize distribution itself and then should be treated with particular care (for pyrene aggregation in small unilamellar vesicles see L’Heureux and Fragata 1989). In view of the above comments on the behavior of  $f$  we might make the following observations. In  $10^{-4} \text{ M}$  phospholipid we get an increase of  $k_1$  with pyrene concentration. This is expected, since in that case and at short times, short  $f$  values suggest very rapid reactions. This is done at the expense of longer-time reaction marking a decrease of  $k_{av}$  at the highest pyrene concentration. In  $3.5 \times 10^{-4} \text{ M}$  phospholipid we got a rather extensive dispersion of  $k_1$  and  $k_{av}$  values, so they may be considered practically invariant, in accordance with the invariance of  $f$  there.

Pyrene was also solubilized in small unilamellar vesicles of  $3.5 \times 10^{-4} \text{ M EPG}$ , at  $20^\circ\text{C}$ . At this temperature,

EPG vesicles are in their liquid crystalline phase. The corresponding anisotropy of the DPH fluorescence (Duportail and Lianos 1990) was 0.10, i.e. the fluidity of their hydrophobic interior is much higher compared with that of DPPG values ( $r=0.33$ ). At very low pyrene concentrations ( $<10^{-6}$  M) we have measured  $\tau_0$  to be 162 ns, in the absence of excimers. This higher decay rate is, apparently, due to unspecific quenching processes owing to the chemical structure of EPG. We have encountered difficulties in our effort to describe the monomer fluorescence decay profiles of pyrene in EPG with (1) or (4). The deconvoluted profiles deviate very little from monoexponentiality and then tend to give an  $f$ -value which is more than 0.9 (cf. Duportail and Lianos 1990). It is obvious that our model finds its limitations when used with this combination of pyrene-EPG at 20°C. Nevertheless, an analysis was carried out using a sum of exponentials and by performing deconvolution. Furthermore, if the fitting is done starting at the 100th channel after the beginning of rise of the excitation pulse (i.e. after 187 ns) the profile is well approximated by a single exponential in the following form

$$I(t) = I_0 \exp [-(k_0 + k[P])t] \quad (5)$$

where  $k$  is an equivalent second-order rate constant. The results of the analysis are given in Table 3. Notice that  $k$  is different at low compared to high pyrene concentration, as expected for inhomogeneous kinetics, even with the simplified model of (6), which implies that we accept excimer formation as the only direction of the reaction, i.e. excimer dissociation is considered negligible. Notice that  $k$  is of the same order of magnitude as the  $k_{av}$ -values obtained with DPPG, but it increases with pyrene concentration. The equivalent first-order  $K = k[P]$ , also shown in Table 3, is also of the same order of magnitude as  $K_{av}$  for DPPG, but it increases to a higher extent for the same pyrene concentration. This behavior of  $k$  and  $K$  marks the greater facility of excimer formation in EPG vesicles owing to their higher fluidity.

Finally, all  $f$  values obtained at 20°C with DPPG are  $<0.67$ , the value of  $f$  for the percolation limit according to Alexander and Orbach (1982). Nevertheless, higher values, above the percolation limit, were obtained at higher temperatures (Table 1). This result might indicate that in the time scale of the present analysis dynamic percolation phenomena are favored at higher temperatures. However, the extremely high values of  $f$  obtained

with EPG vesicles should be seen rather as the extensive relaxation of the imposed geometrical restrictions.

Our results, both with DPPG and EPG vesicles, have shown that pyrene excimer formation in the lipidic core of small unilamellar vesicles can be described by a diffusion model as long as dimensionality considerations are taken into account. Thus the values of the time-exponent  $f$  were allowed to vary both with pyrene concentration and temperature. The previously used model based on Einstein-Smoluchowski diffusion theory (Vanderkooi et Callis 1974) employed a fixed  $f$  equal to 0.5 which applies only to limited cases. The generality of our model is also marked by the fact that it can predict situations of quasi-static excimer formation.

## Conclusion

The kinetics of monomer pyrene in the presence of excimers was studied with time correlated fluorescence in small unilamellar vesicles of DPPG (gel phase) and EPG (liquid crystalline phase). Emphasis was given to the variation of temperature in a range of monophasic DPPG vesicles, as well as to the variation of pyrene concentration. The time exponent  $f$ , calculated during the analysis, gave an estimate of the geometrical restrictions imposed on the reaction. Increase of temperature decreased restrictions and varied reaction rates. Increase of pyrene concentration did not affect  $f$ -values except in the case where the number of solubilizes per vesicle was relatively high allowing for quasi-static interactions. The model of (1) and (4) found its limitations in the system pyrene-EPG at 20°C where the  $f$ -values become very close to 1.0. Classical kinetics can then approximate satisfactorily pyrene excimer formation in such vesicles. The above results help redefining the reaction rate in the vesicle lipidic core and allow the study of reactivity in such environments under new light. They also allow detection of pyrene aggregation in the vesicle lipidic core.

## References

- Alexander S, Orbach R (1982) Density of states on fractals: "fractons". *J Phys Lett* 43:L625-L631
- Allinger K, Blumen A (1980) On the direct energy transfer to moving acceptors. *J Chem Phys* 72:4608-4619
- Argyris P, Kopelman R (1987) Self-stirred vs. well-stirred reaction kinetics. *J Phys Chem* 91:2699-2701
- Argyris P, Duportail G, Lianos P (1991) Behavior of the rate-constant in restricted spaces. *J Chem Phys* 95:9808-9814
- Bartlett GR (1959) Phosphorous assay in column chromatography. *J Biol Chem* 234:466-468
- Blackwell MF, Gounaris K, Barber J (1986) Evidence that pyrene excimer formation in membranes is not diffusion-controlled. *Biophys Biochim Acta* 858:221-234
- Blumen A, Zumofen G, Klafter J (1988) Fractal concepts in reaction kinetics. In: Amann A et al. (eds) *Fractals, quasicrystals, chaos, knots and algebraic quantum mechanics*. Kluwer, London, pp 21-52
- Daems D, van den Zegel M, Boens N, De Schryver FC (1985) Fluorescence decay of pyrene in small and large unilamellar L $\alpha$ -dipalmitoylphosphatidylcholine vesicles above and below the phase transition temperature. *Eur Biophys J* 12:97-105

**Table 3.** Values of the second and first-order rate for excimer formation of pyrene in  $3.5 \times 10^{-4}$  M EPG vs. pyrene concentration at 20°C

Pyrene concentration ( $10^{-6}$ M)	$k$ ( $10^{11}$ M $^{-1}$ s $^{-1}$ )	$K$ ( $10^6$ s $^{-1}$ )
5	1.1	0.6
7.5	2.0	1.5
10	2.8	2.8
15	2.6	4.2
20	2.7	5.4
30	2.9	8.7

- Duportail G, Lianos P (1988) Fractal modeling of pyrene excimer quenching in phospholipid vesicles. *Chem Phys Lett* 149:73–78
- Duportail G, Lianos P (1990) Phospholipid vesicles treated as fractal objects. A fluorescence probe study. *Chem Phys Lett* 165:35–40
- Havlin S, Ben-Avraham D (1987) Diffusion in disordered media. *Adv Phys* 36:695–798
- Kopelman R (1986) Rate processes on fractals: theory, simulations and experiments. *J Stat Phys* 42:185–200
- Klafter J, Blumen A (1984) Fractal behavior in trapping and reaction. *J Chem Phys* 80:875–877
- L'Heureux GP, Fragata M (1989) Monomeric and aggregated pyrene and 16-(1-pyrenyl)hexadecanoic acid in small, unilamellar phosphatidylcholine vesicles and ethanol-buffer solutions. *J Photochem Photobiol* 3:53–63
- Lianos P (1988) Luminescence quenching in organized assemblies treated as media of noninteger dimensions. *J Chem Phys* 89:5237–5241
- Liu BM, Cheung HC, Chen KH, Habercom MS (1980) Fluorescence decay kinetics of pyrene in membrane vesicles. *Biophys Chem* 12:341–355
- Lopez-Quintela MA, Casado J (1989). Revision of the methodology in Enzyme Kinetics: a fractal approach. *J Theor Biol* 139:129–139
- Lopez-Quintela MA, Perez-Moure JC, Bujan-Nunez MC, Samios J (1987) Influence of fractal dimension on diffusion-controlled reactions. *Chem Phys Lett* 138:476–480
- Meakin P, Stanley HE (1984) Novel dimension-independent behavior for diffusive annihilation on percolation fractals. *J Phys A Math Gen* 17:L173–L177
- Rammal R, Toulouse G (1983) Random walks on fractal structures and percolation clusters. *J Phys Lett* 44:L13–L22
- Takami A, Mataga N (1987) Electronic excitation migration and trapping among cationic porphyrins absorbed on anionic vesicle surface. Fractal-like behaviors. *J Phys Chem* 91:618–622
- Yamazaki I, Tamai N, Yamazaki T (1990) Electronic excitation transfer in organized molecular assemblies. *J Phys Chem* 94:516–525
- Vanderkooi JM, Callis JB (1974) Pyrene. A probe of lateral diffusion in the hydrophobic region of membranes. *Biochemistry* 13:4000–4006